PARAMETER OPTIMIZATION DESIGN OF PRECISION SEEDING DEVICE BASED ON THE BP NEURAL NETWORK FOR PANAX NOTOGINSENG

Zhigui Dong[1*], Jiahuai Jiang[1], Yanchao Wang[1]

[1*]Corresponding author. School of Electronic and Information Engineering, Liaoning Institute Science and Technology/Benxi, China.
E-mail: dongzhigui@163.com │ORCID ID: https://orcid.org/0000-0002-4168-7991

ABSTRACT

To address the poor fitness and low accuracy of multiobjective parameter optimization, the BP neural network-based constrained multiobjective optimization method was applied to optimize a seed-metering device. Taking the 2BQ-15 type Panax notoginseng seed-metering device as the research object, the picking hole column diameter, forward velocity, and dropping seed point-to-picking hole roll distance were selected as the experimental factors, and the quality index, missing index and multiple index were selected as the performance indicators. The experimental scheme was designed by the quadratic orthogonal rotation combination, and the BP neural network of the precision seed-metering device was built from the experimental data. The seed-metering device was optimized by the proposed method, and the optimal parameter combinations were obtained as follows: the picking hole column diameter was 27 mm, the forward velocity was 0.50 m/s, and the dropping seed point-to-picking hole roll distance was 330 mm. Under such parameter combinations, the quality index is 93.4%, the missing index is 3.15%, and the multiple index is 3.35%. Finally, a verification test was carried out on the basis of the optimization results, the errors were within the allowable range, and the test results and optimized results were consistent.

INTRODUCTION

Panax notoginseng is a valuable Chinese herbal medicine that is grown in Wenshan City, Yunnan Province, China, and is cultivated by intensive precision seeding. Trenching and precision seeding are two important aspects of the sowing operation, and the performance of the trencher and precision seeding-metering are directly related to the quality of the seeding. The spacing between the rows and plants of Panax notoginseng is approximately 50 mm, so the planting plants are small, and the trenching method is prone to clogging. Compared with traditional trench seeding methods, precision hole seeding disturbs the soil less, making the soil be conducive to soil moisture retention and drought resistance (Lai et al., 2017).

Currently, most of the developed drilling seeders in China use rollers with duckbills, plungers, buckets and other burrowing components as burrowers (Li et al., 2018), which are mainly used for field crops such as maize, wheat, rice and vegetables (Chen & Wang, 2011; Tian et al., 2016). However, the spacing between plants and rows of the existing roller-forming components of the pricking hole is greater than 150 mm (Lai et al., 2019), which cannot meet the agronomic requirements of intensive Panax notoginseng cultivation.

The 2BQ-15 Panax notoginseng seeder (CN107182380A) is a precision seeder designed and developed by Prof. Lai's team at Kunming University of Technology. The operation of the hole seeder meets the agronomic requirements of Panax notoginseng cultivation in terms of plant spacing, row spacing, resowing, missed sowing and other relevant indicators. The quality index, mission index and multiple index are key for measuring the quality of Panax notoginseng precision seeding operations, and these indices are subject to interactions of factors such as the pricking hole column diameter, forward velocity and dropping seed point to the pricking hole roll distance; moreover, the interactions between these factors are unknown. Therefore, optimizing the parameters of the panax notoginseng pricking hole precision seed-metering device is a mechanical optimization design problem with black box characteristics.

The BP neural network-based constrained optimization method is a new approach for the optimization of black box problems and includes single-objective optimization methods and multiobjective optimization methods (Dong et al., 2021; Wang et al., 2017; Dong et al., 2018a; Dong et al., 2019). The proposed method is based on the principle of iterative optimization via mathematical programming methods and the functional relationship fitting of BP neural networks. This method is widely used in many parameter optimization problems in agricultural engineering, such as maize planting patterns (Wang et al., 2017), soybean planting patterns (Dong et al., 2018b; Liang et al., 2020), working parameters for whole straw returning devices (Dong et al., 2018a; Dong et al., 2022), and design parameters for potato planter openers (Zhao et al., 2020).

To address the poor fitness and low accuracy of multiobjective parameter optimization, the accuracy of the 2BQ-25 Panax notoginseng precision seeder was improved, and the agronomic requirements for Panax notoginseng planting were satisfied. In this paper, the BP neural network-based optimization method was applied to optimize the parameters of the hole precision seed-metering device, including the pricking hole column diameter, forward speed, and dropping seed point-to-pricking hole roll distance. To obtain the optimal parameter combination for a hole precision seed-metering device, the qualification index should be improved and the multiple index and missing index should be reduced.

MATERIAL AND METHODS

Structure and working principle of the hole seed-metering device

The Panax notoginseng pricking hole precision seed-metering device is composed of a seed-metering device, a pricking hole roller and a drive mechanism, as shown in Figure 1. The seed-metering system is composed of a seed-metering wheel, brush wheel, seed guard, seed-cleaning knife and shell.
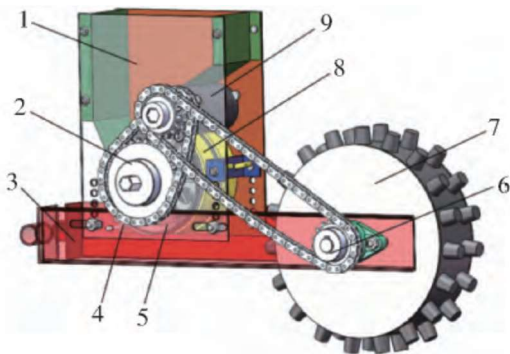
1. shell, 2. Secondary drive mechanism, 3. Connecting frame, 4. Seed-cleaning knife, 5. seed-rowing wheel, 6. Primary drive mechanism, 7. pricking hole roller, 8. seed guard, 9. brush wheel.

FIGURE 1. Structural diagram of the hole seed-metering device.

The pricking hole roller is fixed in the front end of the connecting frame by means of bears and bear blocks, and the seed metering is fixed to the rear end of the connecting frame

by bolts. The dropping seed point-to-the-picking hole roller distance, and the throwing seed height can be adjusted by the bolts. With the rotation of the cavity roller, the primary drive mechanism drives the brush wheel, and the secondary drive mechanism turns the seed-rowing wheel. When the seed-metering device is in operation, the pricking hole roller rolls forward, and holes are pricked through the soil. The seed-metering wheels and brush wheel are rotated by the power transmission of the primary and secondary drive mechanisms, and the extra seeds filled in the hole of the seed-metering wheel are brushed out by a brush to ensure that only one seed is in each hole. With the rotation of the seed-metering wheel, the seed enters the seed protection zone. When the seed reaches the seeding point, it is released from the hole by gravity, and the seed that is not dislodged from the hole is removed by the cleaning knife. The seed is dropped into the hole, and the whole process of seed picking and seed-metering is completed.

Experimental design and methods

To determine the optimal parameter combination, the experiment was designed using a three-factor five-level orthogonal center of rotation combination, experimental factors (features) and codes, as shown in Table 1.

The experimental factors (features) include the picking hole column diameter x_1, the forward velocity x_2, and the dropping seed point-to-picking hole roll distance x_3. According to the results of a single-factor test, the picking hole column diameter (bottom diameter) is 19-35 mm, the forward velocity is 0.25-0.8 m/s, and the dropping seed point-to-pricking hole roll distance is 310-350 mm (Lai et al., 2017).

The performance indicators of the seed-metering device included the qualification index y_1, missing index y_2, and multiple index y_3. According to the methods used for testing single-seed drills (precision drills) (GB/T6973-2005), the quality index, missing index and multiple index are calculated via the following equations.

Qualified index:

$$A = \frac{n_1}{N'} \times 100 \tag{1}$$

Missing index:

$$D = \frac{n_2}{N'} \times 100 \tag{2}$$

Multiple index:

$$M = \frac{n_0}{N'} \times 100 \tag{3}$$

Where:

N' is the number of intervals;

n_1 is the number of qualified individuals;

n_2 is the number of missing individuals, and

n_0 is the number of multiples.

These parameters are calculated according to the methods given in GB/T 6973-2005.

TABLE 1. Experimental factors and codes.

Factors	Codes				
	-1.682	-1	0	1	1.682
pricking hole column diameter/(mm)	19	22	27	32	35
forward velocity/(m/s)	0.25	0.36	0.53	0.69	0.80
dropping seed point-to-the-picking hole roll distance/(mm)	310	318	330	342	350

The BP neural network-based constrained multiobjective optimization method

The constrained multiobjective optimization method based on a BP neural network includes two parts: the construction of the BP neural network model and global optimization. The construction of the BP neural network is divided into two steps: network structure design and network training.

Construction of the BP neural network model

In this paper, the single hidden layer (input layer, hidden layer, and output layer) network structure is selected to design the BP neural network model, and the network structure is shown in Figure 2.
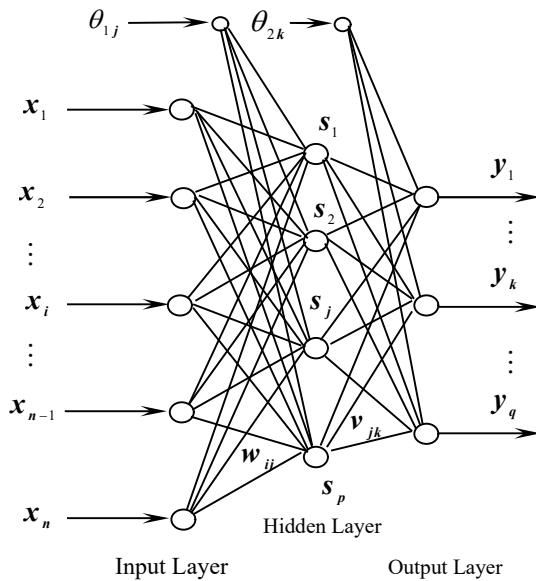

FIGURE 2. Model of a single-hidden-layer BP neural network.

According to the experimental scheme, there are 3 neurons in the input layer, and the input variables (features) are $X=[x_1, x_2, x_3]^T$, where x_1 is the picking hole column diameter, x_2 is the forward velocity, and x_3 is the dropping seed point to-picking hole roll distance. The number of neurons in the output layer is 3, the output variable $Y=[y_1, y_2, y_3]^T$, y_1 is the qualified index, y_2 is the missing index, *and* y_3 is the multiple index. The number of neurons in the hidden layer is 9, which is estimated based on empirical formulae and performance testing. Suppose that W is the weight of the input layer to the hidden layer, V is the weight of the hidden layer to the output layer, and θ_1 and θ_2 are the threshold values for the hidden and output layers, respectively. The unipolar sigmoid function is chosen for the transfer function of the hidden and output layers and is denoted as $f()$. The BP neural network model for the parameter optimization problem of a Panax notoginseng precise seed-metering device can be formulated as follows.

$$Y = F(X) = f[V \cdot f(W \cdot X + \theta_1) + \theta_2] \tag{4}$$

The BP neural network-based constrained multiobjective global optimization method

Ranking the multiple objectives of the parameter optimization problem for the Panax notoginseng precise seed-metering device according to order of importance. Suppose $F_1(X)$ is the main objective, $F_2(X)$ is the secondary objective, and $F_3(X)$ is the third objective. Taking the objective minimization problem as an example, the BP neural network-based constrained multiobjective global optimization method is described.

(1) For the main objective $F_1(X)$, the optimization problem can be expressed as follows:

$$\begin{cases} \min y_1 = F_1(X) = f\left[V \cdot f\left(W \cdot X + \theta_1\right) + \theta_2\right] \\ X \in D \end{cases} \tag{5}$$

Where:

D is the feasible region formed by constraint conditions.

The global optimization method for solving the optimal value F_1^* of the main objective $F_1(X)$ is as follows:

Step 1: Generate an initial point $X(0)$ randomly, $X(0) \in D$. Suppose $X(t)$ is the feasible point obtained in the tth iteration.

Step 2: Calculate the gradient of point $X(t)$ via [eq. (6)]:

$$\frac{\partial F_1(X)}{\partial X}\Big|_{X=X(t)} \qquad t \in [0,1,2,\cdots] \tag{6}$$

Step 3: Judge whether the gradient mode of point $X(t)$ satisfies [eq. (7)].

$$\left\|\frac{\partial F_1(X)}{\partial X}\Big|_{X=X(t)}\right\| = 0 \qquad t \in [0,1,2,\cdots] \tag{7}$$

If this condition is satisfied, $X(t)$ is the optimal solution, and its corresponding network output $F_1(X(t))$ is the optimal value for the main objective. If not, go to Step 4.

Step 4: Calculate the search direction $S(t)$ of point $X(t)$ via Equation (8) and the optimal iteration step length λ along $S(t)$ via [eq. (9)]:

$$S(t) = -\nabla F_1(X(t)) \tag{8}$$

$$\lambda = -\frac{(S(t))^T \nabla F_1(X(t))}{(S(t))^T \nabla^2 F_1(X(t)) S(t)} \tag{9}$$

Where:

$\nabla F_1(X(t))$ is the gradient of point $X(t)$, which can be obtained by the first-order partial derivative of the network output to input,

$\nabla^2 F_1(X(t))$ is the Hesse matrix of point $X(t)$, which can be obtained by the second-order partial derivative of the network output to input.

Step 5: The iterative search is carried out by [eq. (10)], and the new point $X(t+1)$ is obtained

$$X(t+1) = X(t) + \lambda S(t) \tag{10}$$

Step 6: Calculate the values of each constraint function at point $X(t+1)$ and verify the position relationship of the iteration point $X(t+1)$ with respect to the feasible region. If $g_h(X(t+1))$ $(h = 1, 2, \cdots, m)$, point $X(t+1)$ is located within the feasible region formed by the constraint conditions. Let $t=t+1$; then, go to Step 2. If $g_h(X(t+1)) = 0$ $(h = 1, 2, \cdots, m)$, then $g_h(X(t+1)) = 0$ is the functioning constraint function, and point $X(t+1)$ is located at the boundary of the feasible region formed by the constraint function $g_h(X(t+1)) = 0$; then, go to Step 8. If $g_h(X(t+1)) > 0$, then point $X(t+1)$ is located outside the feasible region formed by the constraint conditions; then, go to Step 7.

Step 7: The trial-and-error method was used to adjust the step factor $\lambda(t)$ along the direction $S(t)$; let $\lambda(t) \Leftarrow 0.5\lambda(t)$; and return to Step 5.

Step 8: Let $t=t+1$, calculate the gradient vector $\nabla F_1(X(t))$ of the objective function at point $X(t)$, and calculate the gradient $\nabla g_h(X(t))$ of the functioning constraint function at point $X(t)$; then, test whether point $X(t)$ satisfies

$$\begin{cases} \nabla F_1(X(t)) + \sum_{h=1}^{m} \beta_h \nabla g_h(X(t)) = 0 \\ \beta_h \geq 0 \ (h = 1, 2, \cdots, \ J < m) \end{cases} \tag{11}$$

Where:

$\beta_h \geq 0 \ (h = 1, 2, \cdots, J < m)$ is the Lagrange factor of the hth constraint condition. If the condition is satisfied, the iteration terminates,

$X(t)$ is the optimal solution, and its corresponding network output $F_1(X(t))$ is the optimal value for the main objective. Otherwise, go to Step 9.

Step 9: Calculate the search direction $S(t)$ of point $X(t)$ and iteration step size λ according to eqs (8) and (9). Determine whether λ satisfies $\lambda \leq 0$. If so, $X(t)$ is the optimal solution, and its corresponding network output $F_1(X(t))$ is the optimal value for the main objective. Otherwise, go to Step 2.

(2) For the secondary objective $F_2(X)$, the optimization problem can be expressed as

$$\begin{cases} \min y_2 = F_2(X) = f\left[V \cdot f(W \cdot X + \theta_1) + \theta_2\right] \\ X \in D_1 \subset \left\{X \middle| F_1(X) \leq F_1(X^*) + \varepsilon_1\right\} \end{cases} \tag{12}$$

Where:

ε_1 is the tolerance value. To prevent deviation introduced by the interruption that emerges during problem solving, $\varepsilon_1 \geq 0$.

According to the global optimization method of the main objective $F_1(X)$, the optimal solution $X(t)$ and the optimal value $F_2(X(t))$ of the secondary objective $F_2(X)$ are solved.

(3) For the third objective $F_3(X)$, the optimization problem can be expressed by [eq. (13)]:

$$\begin{cases} \min y_3 = F_3(X) = f\left[V \cdot f(W \cdot X + \theta_1) + \theta_2\right] \\ X \in D_2 \subset \left\{X \middle| F_2(X) \leq F_2(X^*) + \varepsilon_2\right\} \end{cases} \tag{13}$$

Where:

ε_2 is the tolerance value. To prevent deviation introduced by the interruption that emerges during problem solving, $\varepsilon_2 \geq 0$.

According to the global optimization method of the main objective $F_1(X)$, the optimal solution $X(t)$ and the optimal value $F_3(X(t))$ of the third objective $F_3(X)$ are solved. At this time, $X(t)$ is the global optimal solution, and the optimal value $F_3(X(t))$ is the global optimal value of the parameter optimization problem.

RESULTS AND DISCUSSION

Experimental results

According to the test factor coding table, 23 groups of experimental schemes and results (mean value of each sample) are shown in Table 2 (Lai et al., 2017). Two hundred wells in two consecutive rows were counted for each group of experiments; each group of experiments was repeated three times, 69 sample groups were obtained, and the mean value was taken as the test result. The statistical indicators included the number of grains per hole and the depth of the hole.

TABLE 2. Experimental scheme and results (mean value of each sample).

No.	Factors			Experiment results		
	x_1/(mm)	x_2/(m/s)	x_3(mm)	y_1/(%)	y_2/(%)	y_3/(%)
1	-1 (22)	-1 (0.36)	-1 (318)	51.2	23.3	25.5
2	1 (32)	-1 (0.36)	-1 (318)	64.3	19.1	16.6
3	-1 (22)	1 (0.69)	-1 (318)	54.6	25.5	19.9
4	1 (32)	1 (0.69)	-1 (318)	68.5	14.8	16.4
5	-1 (22)	-1 (0.36)	1 (342)	55.3	18.9	25.8
6	1 (32)	-1 (0.36)	1 (342)	82.6	17.0	0.4
7	-1 (22)	1 (0.69)	1 (342)	68.6	14.5	16.7
8	1 (32)	1 (0.69)	1 (342)	84.4	5.6	10.0
9	-1.682 (19)	0 (0.53)	0 (330)	54.3	25.6	23.1
10	1.682 (35)	0 (0.53)	0 (330)	82.7	14.5	2.8
11	0 (27)	-1.682 (0.25)	0 (330)	55.6	23.5	20.9
12	0 (27)	1.682 (0.80)	0 (330)	82.6	1.1	16.3
13	0 (27)	0 (0.53)	-1.682 (310)	56.8	15.9	27.3
14	0 (27)	0 (0.53)	1.682 (350)	83.6	12.8	3.6
15	0 (27)	0 (0.53)	0 (330)	89.7	7.8	2.5
16	0 (27)	0 (0.53)	0 (330)	88.7	9.4	1.9
17	0 (27)	0 (0.53)	0 (330)	92.5	5.8	1.7
18	0 (27)	0 (0.53)	0 (330)	95.5	4.0	0.5
19	0 (27)	0 (0.53)	0 (330)	92.2	6.6	1.2
20	0 (27)	0 (0.53)	0 (330)	84.3	7.9	7.8
21	0 (27)	0 (0.53)	0 (330)	90.2	7.7	2.1
22	0 (27)	0 (0.53)	0 (330)	90.9	5.7	3.4
23	0 (27)	0 (0.53)	0 (330)	93.5	2.2	4.3

Results and analysis of the fitting model based on the BP neural network

Fitted results of the BP neural network model

To determine the network parameters of the optimization model, the computer program was constructed using Python 3.7. The hardware configuration of the experiment is as follows: the processor is an Intel Core i7-4710MQ, the operating system is Windows 10, and the memory size is 16 GB.

Taking the experimental results in Table 2 as the training sample, the normalized interval of the training sample data is [0.3, 0.7], the initial learning rate is 0.7, and the expected accuracy of the network output error is $E=10^{-5}$. The weight matrix of the input and hidden layer W

$$W = \begin{bmatrix} 8.657 & -16.852 & 1.441 & -5.242 & 0.866 & -6.104 & 13.584 \\ -1.427 & 10.899 & -4.106 & 3.672 & 4.640 & -7.829 & -13.471 \\ 5.127 & -1.355 & -12.419 & -5.595 & -0.443 & 3.183 & 0.527 \end{bmatrix}^T$$

Threshold value of the hidden layer θ_1

$$\theta_1 = \begin{bmatrix} -0.883 & -0.348 & -3.323 & 0.110 & 4.105 & -3.774 & -0.709 \end{bmatrix}^T$$

The weight matrix of the hidden and output layers V

$$V = \begin{bmatrix} 4.859 & -4.223 & -10.451 & -1.548 & -9.293 & -4.595 & -2.720 \\ -4.722 & 5.563 & 4.399 & 4.305 & 5.093 & 2.768 & 3.788 \\ -3.496 & 2.013 & 13.107 & -1.245 & 10.362 & 5.009 & 1.032 \end{bmatrix}$$

Threshold value of the hidden layer θ_2

$$\theta_2 = \begin{bmatrix} -0.485 & 0.1935 & 0.811 \end{bmatrix}^T$$

Fitted model analysis of the quality indices and experimental factors

Design-Expert 8.0.6 was applied to process the experimental data, and the regression model was fitted to the qualified indices and experimental data. The analysis of variance (ANOVA) results in Table 3 show that the interaction terms, including the picking hole column diameter and forward velocity, the picking hole column diameter and the dropping seed point to-picking hole roll distance, and the forward velocity and dropping seed point to-picking hole roll distance, were not significantly different (P>0.05). The regression model after excluding nonsignificant factors is

$$y_1 = 90.87 + 8.44x_1 + 8.03x_2 + 7.97x_3 - 8.26x_1^2 - 8.05x_2^2 - 7.66x_3^2$$

(14)

TABLE 3. The analysis of variance.

Source	Qualified index				Missing index				Multiple index			
	SS	DF	F	P	SS	DF	F	P	SS	DF	F	P
Model	5111.1	9	35.54	<0.0001	1137.54	9	12.83	<0.0001	1902.89	9	24.56	<0.0001
x_1	1017.19	1	63.65	<0.0001	144.14	1	14.63	0.0021	453.84	1	52.61	<0.0001
x_2	339.66	1	21.25	0.0005	226.13	1	22.96	0.0004	12.44	1	1.45	0.2507
x_3	694.25	1	43.44	<0.0001	74.58	1	7.57	0.0165	312.79	1	36.34	<0.0001
$x_1 x_2$	14.31	1	0.9	0.3612	22.78	1	2.31	0.1523	72.6	1	7.43	0.0123
$x_1 x_3$	32.4	1	2.03	0.178	2.1	1	0.21	0.6518	48.51	1	5.64	0.0337
$x_2 x_3$	7.03	1	0.44	0.5187	23.46	1	2.28	0.1467	4.96	1	0.58	0.4613
x_1^2	1084.94	1	67.87	<0.0001	412.77	1	41.91	<0.0001	202.94	1	23.58	0.0003
x_2^2	1029.95	1	64.54	<0.0001	88.26	1	8.96	0.0104	493.21	1	57.3	<0.0001
x_3^2	932.85	1	58.37	<0.0001	150.89	1	15.32	0.0018	315.74	1	36.68	<0.0001
bias	207.76	13			128.05	13			111.89	13		
lock of fitted	125.3	2	2.43	0.1267	88.88	2	3.63	0.0519	73.84	2	3.1	0.0751
Error	82.46	8			39.16	8			38.06	8		
Total	5318.85	22			1265.58	22			2014.78	22		

Note: P<0.01, extremely significant. P<0.05, significant. SS: sum of squares. DF: degrees of freedom.

A comparison between the experimental values and the fitted values of the two different models is shown in Figure 3. Figure 3 shows that the BP neural network model has a better fit with the test values than does the regression model. Comparing the coefficient of determination R^2 and the relative mean square error (RMSE) of the two models, the R^2 of the BP neural network model is 0.9845, and the RMSE is 1.95. The R^2 of the regression model is 0.9027, and the RMSE is 3.82. Therefore, the BP neural network model can better reveal the functional relationships between the experimental factors and the quality indices.
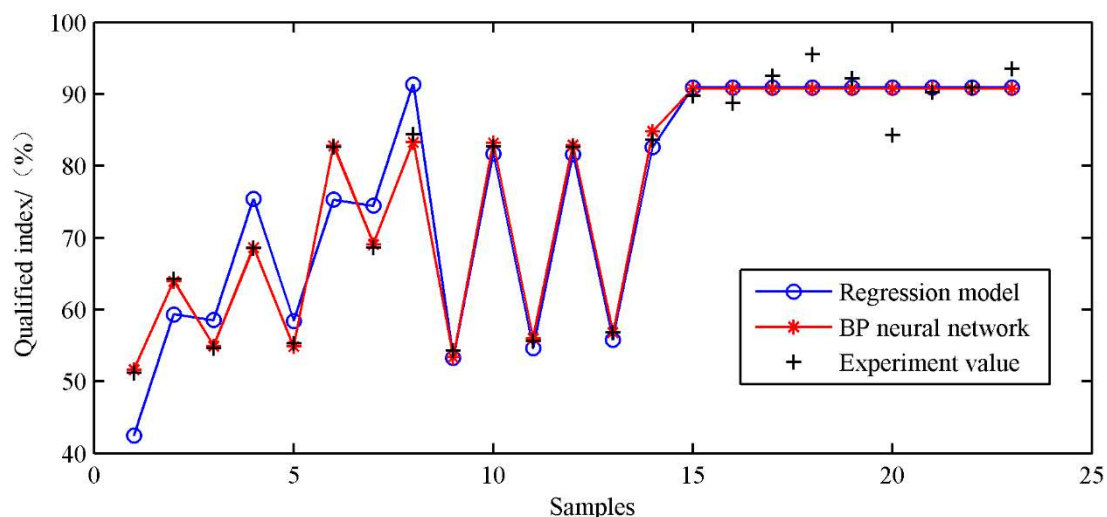

FIGURE 3 Experimental values and fitted values of the BP neural network and regression model.

Fitted model analysis of the missing indices and experimental factors

Design-Expert 8.0.6 was applied to process the experimental data, and the regression model was fitted to the missing indices and experimental data. The ANOVA results revealed that the following interaction terms were nonsignificant (P>0.05): picking hole column diameter and forward velocity, picking hole column diameter and dropping seed point to-picking hole roll distance, and forward velocity and dropping seed point to-picking hole roll distance. The regression model after excluding nonsignificant factors is

$$y_2 = 6.32 - 3.3x_1 - 6.66x_2 - 0.92x_3 + 5.1x_1^2 + 2.36x_2^2 + 3.08x_3^2$$

(15)

A comparison between the experimental values and the fitted values of the two different models is shown in Figure 4. Figure 4 shows that the BP neural network model has a better fit with the test values than does the regression model. Comparing the coefficient of determination R^2 and the relative mean square error (RMSE) of the two models, the R^2 of the BP neural network model is 0.9418, and the RMSE is 0.84. The R^2 of the regression model is 0.8936, and the RMSE is 1.58. Therefore, the BP neural network model can better reveal the functional relationships between the experimental factors and missing indices.
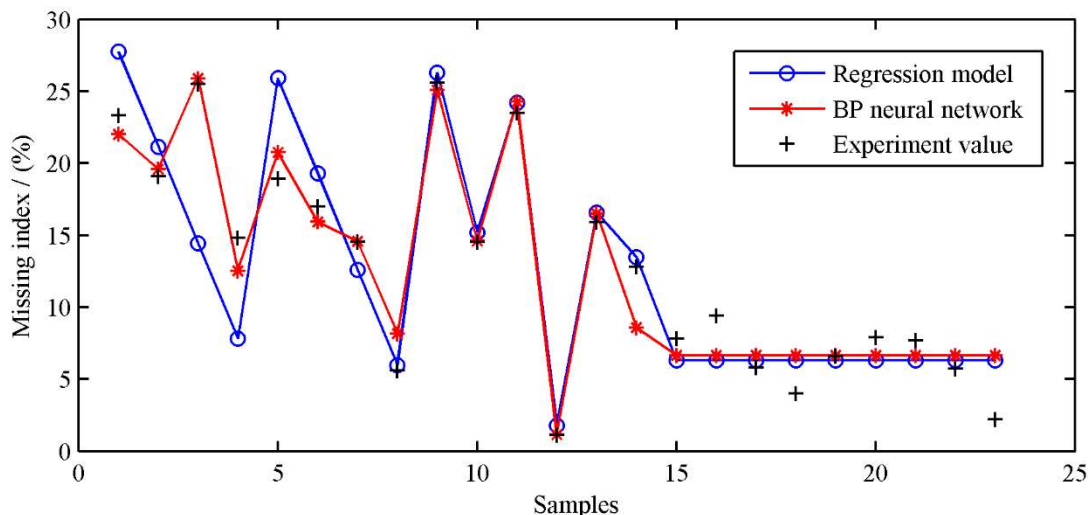

FIGURE 4. Experimental values and fitted values of the BP neural network and regression model.

Fitted model analysis of the multiple index and experimental factors

Design-Expert 8.0.6 was applied to process the experimental data, and the regression model was fitted with the multiple index and experimental data. The ANOVA results revealed that the following parameters were not significantly related (P>0.05): forward velocity, the interaction term between forward velocity and dropping seed point and the picking hole roll distance. The regression model after excluding nonsignificant factors is

$$y_3 = 2.82 - 6.04x_1 - 7.05x_3 + 3.01x_1x_2 - 2.46x_1x_3 + 3.57x_1^2 + 5.57x_2^2 + 4.46x_3^2 \tag{16}$$

A comparison between the experimental values and the fitted values of the two different models is shown in Figure 5. Figure 5 shows that the BP neural network model has a better fit with the test values than does the regression model. Comparing the coefficient of determination R^2 and the relative mean square error (RMSE) of the two models, the R^2 of the BP neural network model is 0.9211, and the RMSE is 0.88. The R^2 of the regression model is 0.8966, and the RMSE is 1.29. Therefore, the BP neural network model can better reveal the functional relationships between experimental factors and multiple indices.
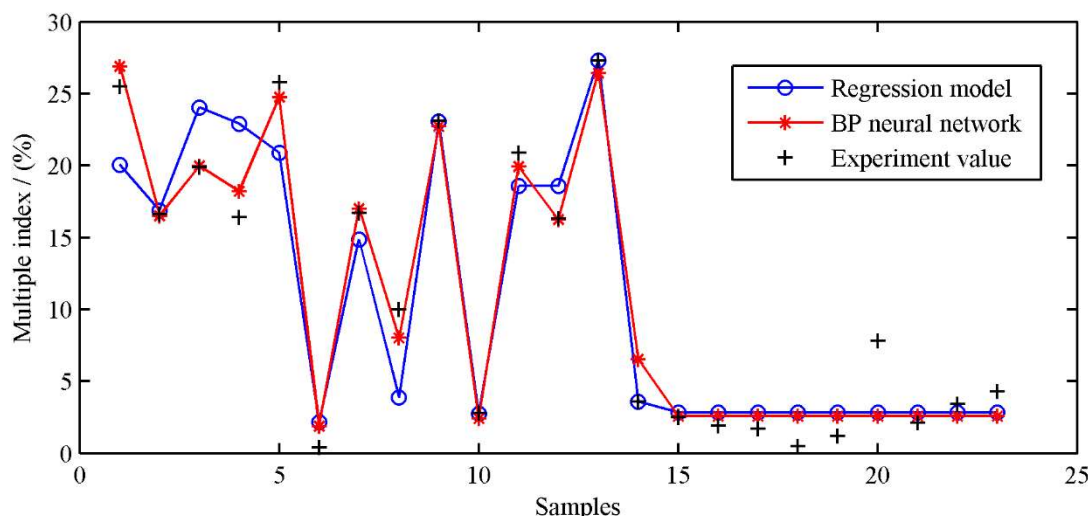

FIGURE 5. Experimental values and fitted values of the BP neural network and regression model.

Global optimization results

The purpose of parameter optimization is to find the optimal parameter combination for determining the picking hole column diameter, forward velocity, and dropping seed point to-picking hole roll distance under the required working conditions, increase the quality index and reduce the missing index and the multiple index. The working performance of the Panax notoginseng precision seeding device must meet the following requirements: a quality index greater than 90%, a missing index and multiple index less than 5%. Therefore, the quality index is the main objective, the missing index is the secondary objective, and the multiple index constitutes the third objective. Taking the fitted BP neural network model as the objective function and the upper and lower limits of the test factors as the constraint conditions, the optimized mathematical model of the quality index was determined.

$$\max \ y_1 = \max \ F_1(\boldsymbol{X}) = f[\boldsymbol{V} \cdot f(\boldsymbol{W} \cdot \boldsymbol{X} + \boldsymbol{\theta}_1) + \boldsymbol{\theta}_2]$$

$$s.t. \begin{cases} 19 \le x_1 \le 35 \\ 0.25 \le x_2 \le 0.80 \\ 310 \le x_3 \le 350 \end{cases} \tag{17}$$

The optimization of the quality index is a problem when finding the maximum objective. First, according to the optimization method given in Section 2.3.2, while the function $-F(\boldsymbol{X})$ obtains the minimum value, the optimal parameter combination is found: the picking hole column diameter is 28.5 mm, the forward velocity is 0.59 m/s, and the dropping seed point-to-picking hole roll distance is 336 mm. The maximum value (94.3%) of the quality index was obtained by $\max F(\boldsymbol{X}) = -\min(-F(\boldsymbol{X}))$.

With a given tolerance of ε_1=0.5, the mathematical model for optimizing the straw return rate as the secondary objective was obtained via [eq. (12)]:

$$\min \ y_2 = \min \ F_2(\boldsymbol{X}) = f[\boldsymbol{V} \cdot f(\boldsymbol{W} \cdot \boldsymbol{X} + \boldsymbol{\theta}_1) + \boldsymbol{\theta}_2]$$

$$s.t. \begin{cases} -F_1(\boldsymbol{X}) \le -94.3 + 0.5 = -93.8 \\ 19 \le x_1 \le 35 \\ 0.25 \le x_2 \le 0.80 \\ 310 \le x_3 \le 350 \end{cases} \tag{18}$$

According to the optimization method given in Section 2.3.2, the mathematical model for missing indices was solved, and the optimal parameter combination was obtained: the picking hole column diameter was 28.0 mm, the forward velocity was 0.55 m/s, and the dropping seed point-to-picking hole roll distance was 325 mm. With this parameter combination, the maximum value of the quality index is 93.8%, and the minimum value of the missing index is 3.1%.

With a given tolerance of ε_2=0.5, the mathematical model for optimizing the straw return rate as the secondary objective was obtained via [eq. (13)]:

$$\min \ y_3 = \min \ F_3(\boldsymbol{X}) = f[\boldsymbol{V} \cdot f(\boldsymbol{W} \cdot \boldsymbol{X} + \boldsymbol{\theta}_1) + \boldsymbol{\theta}_2]$$

$$s.t. \begin{cases} -F_1(\boldsymbol{X}) \le -93.9 + 0.5 = -93.3 \\ F_2(\boldsymbol{X}) \le 3.1 + 0.5 = 3.6 \\ 19 \le x_1 \le 35 \\ 0.25 \le x_2 \le 0.80 \\ 310 \le x_3 \le 350 \end{cases} \tag{19}$$

According to the optimization method given in Section 2.3.2, the optimization mathematical model of multiple indices was solved, and the optimal parameter combination was obtained: the picking hole column diameter was 27.0 mm, the forward velocity was 0.50 m/s, and the dropping seed point-to-picking hole roll distance was 330 mm. With this parameter combination, the maximum value of the quality index is 93.4%, the minimum value of the missing index is 3.1%, and the multiple index is 3.35%.

Verification test

To verify the correctness of the optimization results obtained by the optimization method in this paper, the performance indices of the seed-metering devices were evaluated by testing the whole machine of the 2BQ-15 type Panax notoginseng precision seed-metering device. The verification test was conducted at Kunming University of Science and Technology in October 2022. The following parameters were used for the experiment: the picking hole column diameter was 27.0 mm, the forward velocity was 0.50 m/s, and the distance from the dropping seeds to-picking hole roll was 330 mm. The cells in each group of 200 wells in two rows were counted, and each group was replicated five times. The average value was taken as the experimental result and is shown in Table 4.

TABLE 4. Optimization result verification based on the BP neural network.

Indices	Minimum value	Maximum value	Mean value	Theoretical value	Relative error
qualified index/(%)	93.1	95.2	93.6	93.4	0.21
missing index/(%)	3.02	3.27	3.17	3.15	0.63
multiple index/(%)	3.21	3.53	3.39	3.35	1.19

Table 4 shows that in the verification test, the average value of the quality index is 93.6%, reflecting a relative error of 0.21% compared with the theoretical results. The average value of the missing indices is 3.17%, with a relative error of 0.63% compared with the theoretical results. The average value of the multiple index is 3.39%, with a relative error of 1.19% compared with the theoretical results. Although there is a certain error between the test results and the theoretical results, considering the comprehensive impact of factors such as the water content of the test plots and flatness, the error in the test results is within the allowable range. Therefore, the results of the verification test were consistent with the optimized results obtained by the optimization method, and the optimized results obtained by the BP neural network were accurate and reliable (Dong et al., 2022).

CONCLUSIONS

The performance indicator of the BP neural network model between the experimental factors and the performance indicators is better than that of the regression model, which can explain the influence of the experimental conditions well.

The optimization combination was obtained by the BP neural network-based multiobjective constrained optimization method under the following experimental conditions: the picking hole column diameter was 27 mm, the forward velocity was 0.50 m/s, and the dropping seed point-to-picking hole roll distance was 330 mm. Under such parameter combinations, the quality index is 93.4%, the missing index is 3.15%, and the multiple index is 3.35%. As the test parameters, the verification test was verified by taking the optimization results, and the verification test results showed that the test results and optimized results were consistent.

The proposed method was applied to optimize a Panax notoginseng precision seed-metering device. This method is important for guiding the design of precision seed-metering devices and provides a new method for similar optimization problems.

REFERENCES

Chen XG, Wang M (2011) Study on key factors of the duckbill punch roller-type pneumatic metering device. Journal of Agricultural Mechanization Research 33(3): 30-37. https://doi.org/10.13427/j.cnki.njyi.2011.03.019

Dong ZG, Song QF, Wang FL (2019) An Unconstrained optimization method based on BP neural network. Statistics and Decision 35(1):79-82. https://doi.org/10.13546/j.cnki.tjyjc.2019.01.017

Dong ZG, Song QF, Wang FL, Wu ZH, Li ZY (2018a) Optimize on power dissipation of rice straw whole straw returning device based on BP neural network. Systems Engineering Theory and Practice 38(9): 2401-2408. https://doi.org/10.12011/1000-6788(2018)09-2401-08

Dong ZG, Song QF, Zhang W (2022) Parameter optimization of whole-straw returning device based on the bp neural network. Engenharia Agrícola 42(4): e20210208. https://doi.org/10.1590/1809-4430-Eng.Agric.v42n4e20210208/2022

Dong ZG, Wu CY, Fu XS, Wang FL (2021) Research and application of back propagation neural network-based linear constrained optimization method. IEEE Access 09:126579-126594. https://doi.org/10.1109/ACCESS.2021.3111900

Dong, ZG, Wang FL, Song QF, Wu ZH, Wang HP (2018b) Optimization of soybean planting density and fertilizing amount based on BP neural network. International Agricultural Engineering Journal 27(3): 28-35.

Lai QH, Cao XL, Yu QX, Sun K, Qin W (2019) Design and experiment of precision seeding device for hole-drop planter for Panax notoginseng. Transactions of the Chinese Society for Agricultural Machinery 50(1):85-95. https://doi.org/10.6041/j.issn.1000-1298.2019.01.009

Lai QH, Ma WP, Liu S, Su W, Zhang ZH (2017) Simulation and experiment on seed-filling performance of pneumatic disc seed metering device for mini-tuber. Transactions of the Chinese Society for Agricultural machinery 48(5): 44-53. https://doi.org/10.6041/j.issn.1000-1298.2017.05.005

Li MT, Li TY, Guan XD, Zhao GK, Zhou FJ (2018) Mechanism design and experiment of rotary hole seeder for dryland. Transactions of the Chinese Society for Agricultural Machinery 49(2):48-57. https://doi.org/10.6041/j.issn.1000-1298.2018. 02.007

Liang XG, Zhao HL, Wang FL, Dong ZG (2020) Optimization of soybean planting density and fertilizer application rate based on RBF neural network. Soybean Science 39(3): 406-413. https://doi.org/10.11861/j.issn.1000-9841.2020.03.0406

Tian LQ, Wang JQ, Tang H, Li SW, Zhou WQ, Shen HG (2016) Design and performance experiment of helix grooved rice seeding device. Transactions of the Chinese Society for Agricultural Machinery 47(5): 46-52. https://doi.org/10.6041/j.issn.1000-1298.2016.05.007

Wang FL, Dong ZG, Wu ZH, Fang K (2017) Optimization of maize planting density and fertilizer quantity based on BP neural network. Transactions of the Chinese Society of Agricultural Engineering 33(6): 92-98. https://doi.org/10.11975/j.issn.1002-6819. 2017.06.012

Zhao SX, Dong ZG, Liu QL, Zhou DL (2020) Optimization of soil returning quantity of the furrow opener of potato planter based on BP neural network. International Agricultural Engineering Journal 29(2): 423-429.